

# Breakdown Properties of Polyethylene Nanocomposites Containing Calcined Zirconia

Khalida Razalie<sup>1,2,\*</sup>, Kwan Yiew Lau<sup>1,\*</sup> and Noor Syazwani Mansor<sup>1</sup>

<sup>1</sup>Faculty of Electrical Engineering, Universiti Teknologi Malaysia, 81310 UTM Skudai, Johor, Malaysia.

<sup>2</sup>Department of TVET Electrical, Sarawak Skills, Kuching, Sarawak.

\*Corresponding author: khalida@sarawakskills.edu, kwanyiew@utm.my

**Abstract:** Electrical insulation is vital in high voltage apparatuses. The most common materials used in commercial high voltage power cable insulation are polymers such as low-density polyethylene (LDPE) and cross-linked polyethylene (XLPE). Nevertheless, these insulation materials have their own advantages and disadvantages. The use of LDPE alone, for example, could not sustain high operating temperatures. Meanwhile, XLPE insulation has crosslinking byproducts that cause degradation of the material especially in the long run. Therefore, PE blends such as LDPE and HDPE blends have been proposed to exhibit material characteristics having good comprises. The composition of 80% LDPE and 20% HDPE often gives desirable results in the flexibility and dielectric properties of the material. Consequently, polymer nanocomposites have been proposed to enhance the performance of LDPE/HDPE blend power cable insulation materials. Although the addition of nanofillers to polymers can enhance the dielectric properties of nanocomposites, it can also otherwise degrade the dielectric properties of nanocomposites, especially the breakdown strength. The current work was conducted to investigate the effects of calcined zirconia ( $ZrO_2$ ) on the breakdown properties of polyethylene (PE) nanocomposites. The  $ZrO_2$  nanopowder used was uncalcined, calcined at 900 °C, and calcined at 1100 °C, to determine these effects on the breakdown strength of PE/ $ZrO_2$  nanocomposites. The results showed that PE/ $ZrO_2$  nanocomposites possessed similar breakdown strength to unfilled PE when  $ZrO_2$  was uncalcined and calcined at 900 °C. Nevertheless, calcining  $ZrO_2$  at 1100 °C led to a slight reduction in the breakdown strength of PE/ $ZrO_2$  nanocomposites compared to unfilled PE. This was ascribed to the agglomeration of  $ZrO_2$  upon calcining at 1100 °C. Therefore, nanofiller calcination temperatures had effects toward the breakdown strength of the final nanocomposites.

**Keywords:** breakdown, calcination, zirconia, polymers, nanocomposites

© 2024 Penerbit UTM Press. All rights reserved

*Article History: received 30 June 2024; accepted 2 December 2024; published 30 December 2024*

## 1. INTRODUCTION

An electrical insulation system is a vital element in every electrical and electronic device. The main purpose of the insulation is to cover an electrical conductor and to prevent electricity from leaking out. All electrical devices, either small or big, must have proper insulation systems. There is no exception to the electrical power industry involving the use of low voltage (LV), medium voltage (MV), high voltage (HV), and extra high voltage (EHV) electricity. Hence, the fire safety of high voltage (HV) outdoor insulator is to maintenance the reliable operation of the electrical grid. Generally, higher voltage levels require better insulation systems over lower voltage levels [1-3].

Polyethylene (PE) and cross-linked polyethylene (XLPE) are widely utilized as insulating materials in high voltage insulation apparatuses especially because both of these materials have low dielectric losses [4]. PE is a thermoplastic polymer with variable crystalline structure. There are varieties of PE, which consists high-density polyethylene (HDPE), low-density polyethylene (LDPE), and linear low density polyethylene (LLDPE). These commodity plastics are produced by addition or radical polymerization. These materials are widely used not only

for power cable insulation, but also for plastic containers, bottles, bags, and plastic toys [5].

Power cable insulation materials could consist of rubbers, dry papers and polymers. Currently, the most common materials used for commercial high voltage direct current (HVDC) [6] and high voltage alternating current (HVAC) power cables are polymers such as LDPE, a combination of HDPE and LDPE with different compositions, and XLPE [7-13]. Nevertheless, each of these insulation materials have their own advantages and disadvantages.

Recently, polymer nanocomposites have been proposed to enhance the performance of conventional power cable insulation materials. This is because nanocomposites exhibit unique electrical properties, even with the addition of low nanofiller loading levels (not more than 10 wt%). Although the addition of nanofillers to polymers can enhance the dielectric properties of nanocomposites, it can also otherwise degrade the dielectric properties of nanocomposites, especially the breakdown strength [14, 15]. For example, Du et al. [16] reported 5% reduction of DC breakdown strength in polypropylene added with 2 wt% of ZnO. The reduction

was caused by lower crystallization temperature and crystallinity of nanocomposites containing ZnO [16].

The existence of the interface area in nanocomposites generally affects the dielectric properties of the materials. Of note, the interface area could also become an attraction place for water to accumulate, especially when polymers are added with oxide-based nanofillers. According to Hosier et al. [15], the existence of oxide groups on the surface of nanofillers added to polymers caused water to reside within the interphase of nanocomposites. For single metal oxide nanoparticles, water is generally present in the form of concentric circle. This phenomenon is regarded as water shell [17]. Hui et al. [17] claimed that higher loading levels of nanofillers led to higher specific surface area affecting the hydration level in nanocomposites. Therefore, the water shell thickness was highly subject to the hydration level [17]. Lau et al. [18] claimed that PE with silica (SiO<sub>2</sub>) generally absorbed more water compared to unfilled PE. This consequently increased the permittivity and loss tangent of PE added with SiO<sub>2</sub>. From the conducted experiment, PE with 2 wt% of SiO<sub>2</sub> absorbed more water (about 0.3%) after being immersed in water for 30 days as compared to unfilled PE, which only absorbed 0.02% of water [18].

To reduce the water content in nanoparticles, calcination of nanoparticles can be applied. Calcination is a high temperature heating process, where the physical and chemical changes in nanoparticles can happen after the calcination process [19]. According to Mayabadi et al. [20], the calcination process brought a positive impact to tin oxide (SnO<sub>2</sub>)/titanium oxide (TiO<sub>2</sub>) nanocomposites for optical and photo electrochemical research applications. The calcination process was done in air for 2 h at 200 °C and the results showed that TiO<sub>2</sub> nanofiller with different properties could be tailored by controlling the morphology of TiO<sub>2</sub> through calcination.

In the current work, we report on the effect of zirconia (ZrO<sub>2</sub>) calcination on the breakdown properties of PE nanocomposites. ZrO<sub>2</sub> was chosen as it is a common type of nanofiller shown to be encouraging in enhancing electrical properties of nanocomposites, if adequately engineered [21]. Three types of ZrO<sub>2</sub> were investigated, i.e., uncalcined ZrO<sub>2</sub>, ZrO<sub>2</sub> calcined at 900 °C, and ZrO<sub>2</sub> calcined at 1100 °C, at 0.5 wt%, 1 wt%, and 3 wt% addition to PE. The breakdown properties of PE/ZrO<sub>2</sub> nanocomposites with respect to the calcination temperatures and nanofiller amounts are discussed.

## 2. EXPERIMENTAL

### 2.1 Materials and Blending

PE consisted of 80% LDPE (Titanlene LDF200YZ) and 20% HDPE (Titanlene HI2000) was used as the base PE in this research. Both the LDPE and HDPE were manufactured by Lotte Chemical Titan. Meanwhile, ZrO<sub>2</sub> was obtained from Sigma Aldrich and used as a nanofiller. The nanofiller was from the oxide-based category, with particle size of 20 nm.

### 2.2 Filler Calcination

ZrO<sub>2</sub> nanopowder was calcined in a Carbolite Gero CWF 13/5 chamber furnace. Several calcination temperatures were chosen to determine the effects of ZrO<sub>2</sub> nanopowder on PE after calcination. This resulted in three types of

ZrO<sub>2</sub>, i.e., uncalcined ZrO<sub>2</sub>, ZrO<sub>2</sub> calcined at 900 °C, and ZrO<sub>2</sub> calcined at 1100 °C.

ZrO<sub>2</sub> nanopowder was first weighed using the Ohaus Pioner laboratory balance to measure the mass of the nanopowder. The nanopowder was then placed in a crucible for calcination in the chamber furnace. The furnace's setpoint ramp rate was specified at 25 °C min<sup>-1</sup> to reach the intended calcination temperature. The nanopowder sample was then calcined for 6 h before it experienced a natural cool down for about 12 h.

### 2.3 Preparation of Nanocomposites

The formulation of PE nanocomposites with ZrO<sub>2</sub> nanofillers (uncalcined ZrO<sub>2</sub>, ZrO<sub>2</sub> calcined at 900 °C, and ZrO<sub>2</sub> calcined at 1100 °C) was prepared using a Brabender mixer. The duration, speed, and temperature were set at 10 min, 55 rpm, and 170 °C. Three nanofiller levels were chosen to be added to the base polymer, i.e., 0.5 wt%, 1 wt%, and 3 wt%.

A Carver hydraulic laboratory hot press was used to produce thin film samples. First, the temperature of the hot press was set at 170 °C. Then, the blended materials were cut into small pieces. Next, the materials were placed in between two Melinex films and sandwiched between two metal plates before being inserted into the hydraulic laboratory hot press. A load of 2.5 ton was then applied to produce an approximately 100 µm thickness of each melt-pressed sample with a diameter approximately 80 mm. To avoid all samples from absorbing environmental water, the samples were kept in a desiccator until use.

The F/A/C notation was used to indicate each sample type. In this, F defines the type of filler, A denotes the amount of the filler, and C represents the calcination temperature of the filler. Table 1 shows the produced test samples and their designations.

Table 1. Sample Designation

Sample Designation (F/A/C)	Nanofiller (F)	Amount of Nanofiller (A)	Calcination Temperature (C)
U/0/0	No nanofiller	0 wt%	Untreated
Z/0.5/0	ZrO <sub>2</sub>	0.5 wt%	Untreated
Z/1/0	ZrO <sub>2</sub>	1 wt%	Untreated
Z/3/0	ZrO <sub>2</sub>	3 wt%	Untreated
C/0.5/900	ZrO <sub>2</sub>	0.5 wt%	900 °C
C/1/900	ZrO <sub>2</sub>	1 wt%	900 °C
C/3/900	ZrO <sub>2</sub>	3 wt%	900 °C
C/0.5/1100	ZrO <sub>2</sub>	0.5 wt%	1100 °C
C/1/1100	ZrO <sub>2</sub>	1 wt%	1100 °C
C/3/1100	ZrO <sub>2</sub>	3 wt%	1100 °C

### 2.4 Differential Scanning Calorimetry

To characterize the melting behavior of all samples, Perkin Elmer differential scanning calorimeter (DSC) 7 that came with Pyris software was used. A sample of about 5 mg in mass was placed in a sealed aluminum pan for measurement purposes. Under a nitrogen atmosphere with a scan rate 10 °C min<sup>-1</sup>, the sample was heated from temperature 30 °C to 160 °C temperature. For calibration purposes, high purity indium, with a known melting temperature of 156.6 °C and melting enthalpy of 28.45 Jg<sup>-1</sup> was used. The reproducibility of measurements was estimated based on the repeated measurements conducted from the same batch of test samples.

## 2.5 Electrical Breakdown

An alternating current (AC) breakdown test was conducted to determine the electrical properties of the prepared samples. The standard referred to conduct the AC breakdown test was American Society for Testing and Materials (ASTM) D149. The test was conducted to determine the dielectric breakdown strength through the thickness of the test sample (puncture). A Baur PGK 110HB AC high voltage test set, with a rated voltage of 80 kV, was used. For every testing, a 100  $\mu\text{m}$  thick sample was placed in between two 6.3 mm diameter spherical ball electrodes immersed in silicone oil to prevent surface flashover. A step voltage of 1 kV every 20 s was applied under room temperature for AC breakdown test. 15 breakdown tests were conducted on each material system, and the breakdown strength was calculated using equation (1). All the measurement data were analyzed using the two-parameter Weibull distribution method. The schematic diagram for the AC breakdown test is shown in Figure 1.

$$\text{Breakdown strength (kVmm}^{-1}\text{)} = \frac{\text{Breakdown voltage (kV)}}{\text{Thickness of sample (mm)}} \quad (1)$$

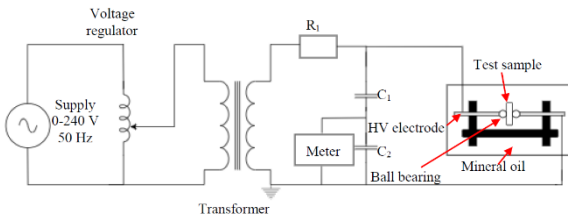


Figure 1. Schematic diagram for AC breakdown test [22]

## 3. RESULTS AND DISCUSSION

### 3.1 Differential Scanning Calorimetry

Figure 2 shows the DSC melting behaviours of unfilled PE and PE nanocomposites that contained 0.5 wt%, 1 wt%, and 3 wt% of uncalcined  $\text{ZrO}_2$  (Z/0.5/0, Z/1/0, and Z/3/0). From the result obtained, the melting behaviours of all nanocomposites and unfilled PE were comparable. The melting peaks could be categorized to three types, namely, the lower melting peak, the intermediate melting peak, and the upper melting peak. Notably, the melting trace of LDPE at 106  $^{\circ}\text{C}$  could be observed from the lower melting peak while the melting trace for HDPE could be observed from the upper melting peak at 125  $^{\circ}\text{C}$ . This is in line with the used of PE blend with ratio 80:20 (LDPE:HDPE). The upper melting peak corresponds to the fusion peak of the  $\alpha$ -crystal form of HDPE while the lower melting peak corresponds to the melting trace of LDPE [23]. Meanwhile, the intermediate melting peak lied between 119  $^{\circ}\text{C}$  and 120  $^{\circ}\text{C}$ , which represented the co-crystallisation of LDPE and HDPE within the PE blend system [23, 24]. These DSC melting behaviors were similar to previously investigated work [24].

Meanwhile the samples of DSC cooling traces are shown in Figure 3. All samples are characterized by a crystallization Temperature ( $T_c$ ) close to 112  $^{\circ}\text{C}$ . This is in line with the previous finding [25]. It is noteworthy that the underlying lamellar structure of materials was not affected by the addition of  $\text{ZrO}_2$ .

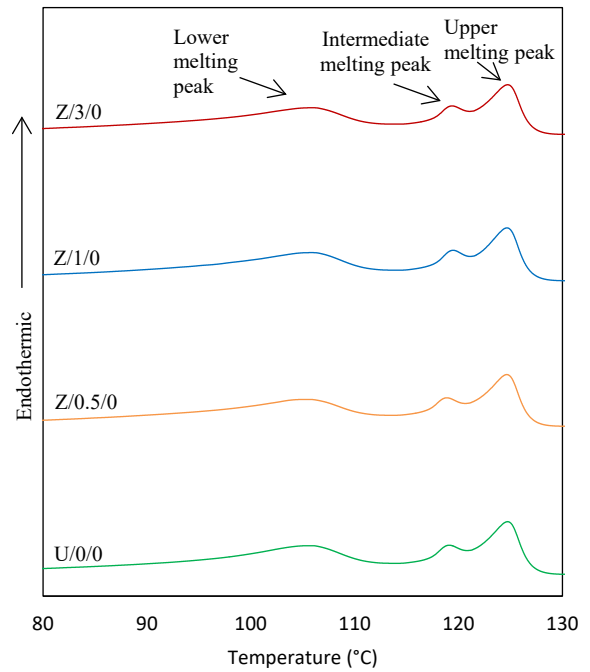


Figure 2. DSC melting traces of U/0/0, Z/0.5/0, Z/1/0, and Z/3/0

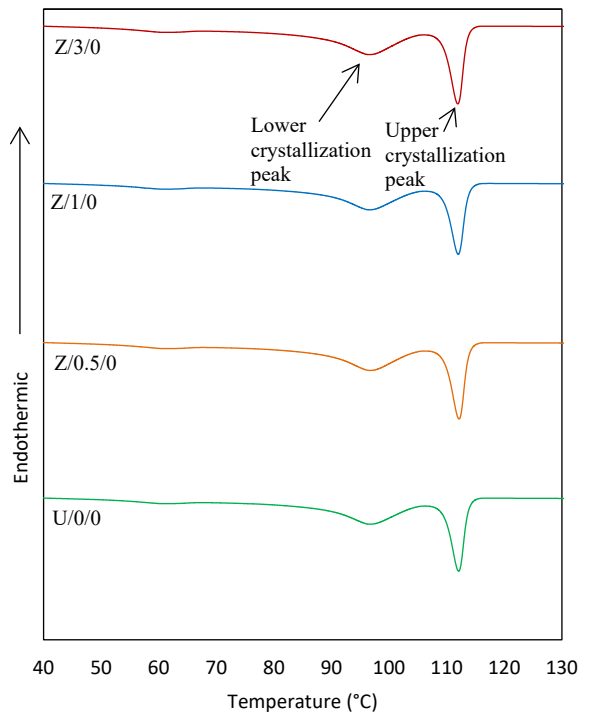


Figure 3. DSC cooling traces of U/0/0, Z/0.5/0, Z/1/0, and Z/3/0

### 3.2 AC Breakdown Strength

Figure 4 shows the Weibull plots of AC breakdown strength for unfilled PE (U/0/0) and nanocomposites that contained uncalcined  $\text{ZrO}_2$  of 0.5 wt% (Z/0.5/0), 1 wt% (Z/1/0), and 3 wt% (Z/3/0). The breakdown value for U/0/0 was 153  $\text{kV mm}^{-1}$  (see Table 2 for details). Meanwhile, the AC breakdown value for Z/0.5/0 was 162  $\text{kV mm}^{-1}$ .

For Z/1/0, its AC breakdown value was 153 kV mm<sup>-1</sup>. Finally for Z/3/0, its AC breakdown value was 146 kV mm<sup>-1</sup>. Considering Weibull uncertainties, the AC breakdown strength of Z/0.5/0, Z/1/0, and Z/3/0 was comparable to U/0/0, albeit that it appeared that the

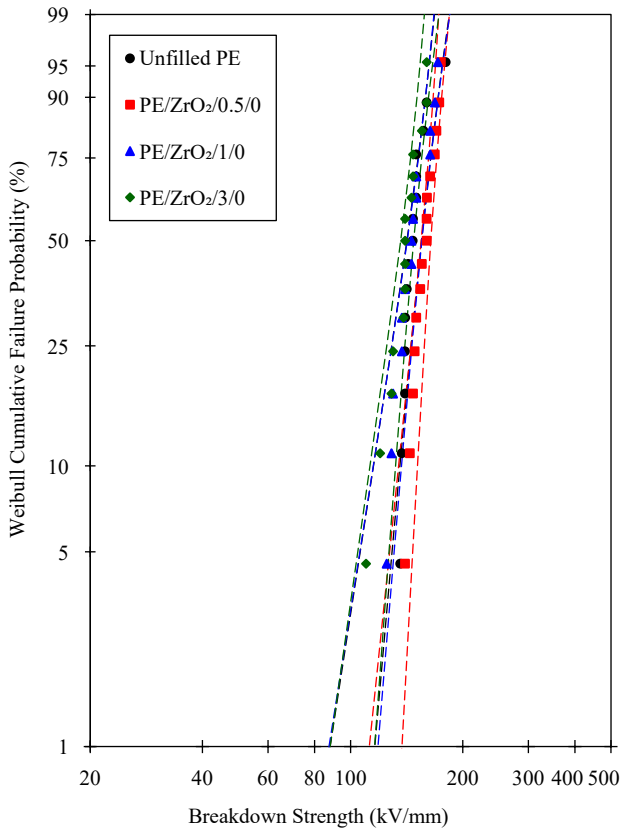


Figure 4. Comparison of AC breakdown strength of U/0/0, Z/0.5/0, Z/1/0, and Z/3/0 based on Weibull plots

Table 2. AC Breakdown Parameter

Sample Designation (F/A/C)	Scale parameter, $\alpha$ (kV mm <sup>-1</sup> )	Shape parameter, $\beta$
U/0/0	153 ± 7	11 ± 4
Z/0.5/0	162 ± 8	16 ± 4
Z/1/0	153 ± 6	11 ± 3
Z/3/0	146 ± 6	12 ± 4
Z/0.5/900	150 ± 3	17 ± 5
Z/1/900	153 ± 5	12 ± 4
Z/3/900	139 ± 3	16 ± 5
Z/0.5/1100	143 ± 7	8 ± 2
Z/1/1100	142 ± 6	10 ± 3
Z/3/1100	140 ± 3	8 ± 2

breakdown strength of the nanocomposites reduced with increasing amounts of ZrO<sub>2</sub>.

The Weibull plots of AC breakdown strength for nanocomposites that contained 0.5 wt% (Z/0.5/900), 1 wt% (Z/1/900), and 3 wt% (Z/3/900) of ZrO<sub>2</sub> calcined at 900 °C are shown in Figure 5. The breakdown strength of Z/0/0, Z/0.5/900, and Z/1/900 were not significantly different from each other when taking Weibull uncertainties into account. At 3 wt% of ZrO<sub>2</sub> loading, however, the breakdown strength of Z/3/900 appeared slightly lowered than U/0/0. Nevertheless, when comparing the breakdown strength of the nanocomposites that contained uncalcined ZrO<sub>2</sub> and ZrO<sub>2</sub> calcined at 900

°C at equivalent ZrO<sub>2</sub> loading levels, the breakdown values appeared indistinguishable.

Therefore, under AC field, the addition of uncalcined ZrO<sub>2</sub> to PE did not significantly affect the breakdown strength of the nanocomposites compared to unfilled PE. Similarly, adding ZrO<sub>2</sub> calcined at 900 °C to PE did not significantly affect the breakdown strength of the final

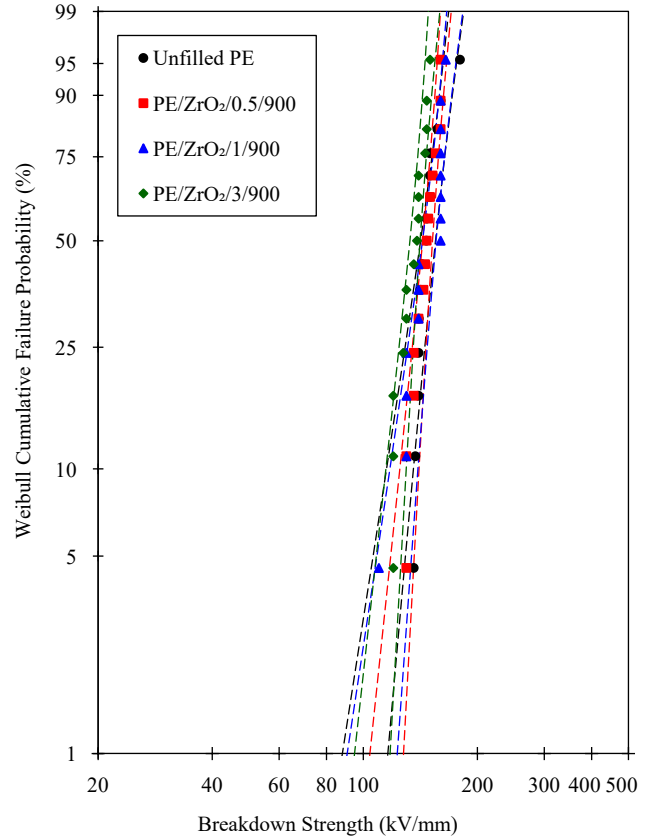


Figure 5. Comparison of AC breakdown strength of U/0/0, Z/0.5/900, Z/1/900, and Z/3/900 based on Weibull plots

nanocomposites. Similar results were reported by Rahim et al. [26], where the effects of nanofiller and nanofiller calcination at 900 °C were less influential on the breakdown strength under AC fields [17].

Figure 6 shows the Weibull plots of AC breakdown strength for nanocomposites that contained 0.5 wt% (Z/0.5/1100), 1 wt% (Z/1/1100), and 3 wt% (Z/3/1100) of ZrO<sub>2</sub> calcined at 1100 °C. The value of AC breakdown strength for Z/0.5/1100 decreased by 12% to 143 kV mm<sup>-1</sup> compared to its uncalcined counterpart (162 kV mm<sup>-1</sup>). The value for Z/1/1100 was also decreased, by 7% to 142 kV mm<sup>-1</sup>, compared to its uncalcined counterpart (153 kV mm<sup>-1</sup>). Lastly, the breakdown value for Z/3/1100 was slightly decreased by 4% to 140 kV mm<sup>-1</sup> compared to its uncalcined counterpart (146 kV mm<sup>-1</sup>). These show that calcining ZrO<sub>2</sub> at a higher temperature, i.e., 1100 °C, appeared to lead to unfavorable breakdown performance of the final materials.

Zamani et al. [27] suggested that, when increasing the nanofiller calcination temperature from 900 °C to 1100 °C, ZrO<sub>2</sub> nanoparticles tended to agglomerate, thus decreasing the surface area of the nanoparticles. The findings by Zamani et. al [27] are consistent with the work reported

here. It is therefore believed that calcining  $ZrO_2$  at  $1100^\circ C$  in the current work led to the agglomeration of  $ZrO_2$ , which slightly reduced the breakdown value of PE that contained  $ZrO_2$  calcined at  $1100^\circ C$ , albeit that such effect is less apparent under AC field. To further understand the effect of  $ZrO_2$  calcination, more work is currently being carried out, especially in determining the structure of the materials and the effect of  $ZrO_2$  calcination on the direct current (DC) breakdown strength of the final nanocomposites.

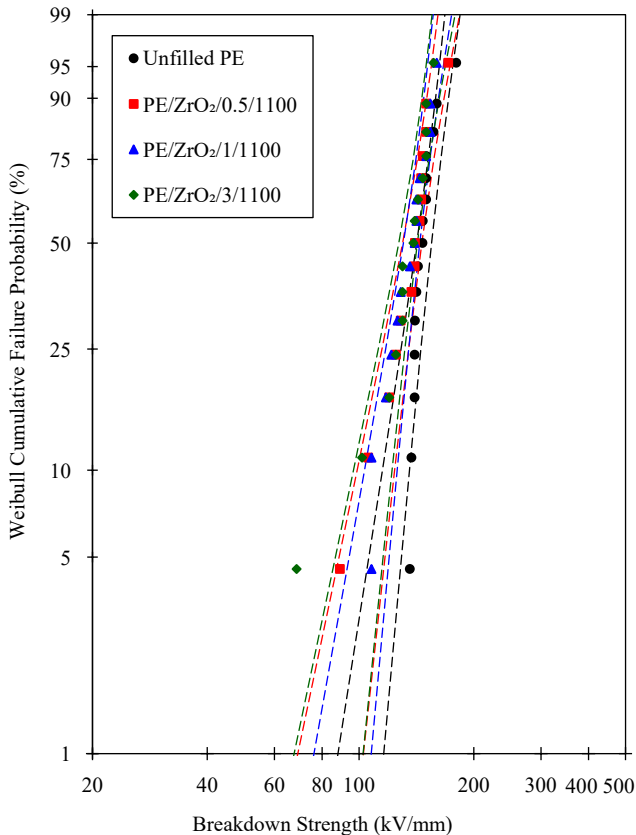


Figure 6. Comparison of AC breakdown strength of U/0/0, Z/0.5/1100, Z/1/1100, and Z/3/1100 based on Weibull plots

#### 4. CONCLUSION

In the work reported here, PE nanocomposites that contained 0.5 wt%, 1 wt%, and 3 wt% of uncalcined  $ZrO_2$  and  $ZrO_2$  calcined at  $900^\circ C$  showed insignificant difference in their AC breakdown strength compared to the unfilled PE. However, increasing the  $ZrO_2$  calcination temperature to  $1100^\circ C$  appeared to slightly decrease the AC breakdown strength of the final nanocomposites. When nanopowder was calcined at  $1100^\circ C$ ,  $ZrO_2$  nanoparticles tended to agglomerate, thus decreasing the surface area of the nanoparticle. Calcining  $ZrO_2$  nanopowder at  $1100^\circ C$  therefore led to the agglomeration of  $ZrO_2$ . Subsequently, the AC breakdown strength of PE that contained  $ZrO_2$  calcined at  $1100^\circ C$  reduced by 7% compared to equivalent PE nanocomposites that contained  $ZrO_2$  calcined at  $900^\circ C$ . Therefore, nanofiller calcination temperatures somehow have effects toward the AC breakdown strength of the final nanocomposites. Overall, the current work demonstrates that the breakdown

properties of PE nanocomposites are dependent not only on the weight percentage of nanofiller loadings, but also on the type of nanofiller, i.e., the calcination temperature of nanofiller.

#### ACKNOWLEDGMENTS

The authors acknowledge Sarawak Skills and Yayasan Sarawak for providing financial sponsorships. The authors also thank the Ministry of Higher Education Malaysia and Universiti Teknologi Malaysia for supporting the research through the respective Fundamental Research Grant Scheme (FRGS/1/2023/TK07/UTM/02/5) and the UTM Fundamental Research Grant (Q.J130000.3823.22H34).

#### REFERENCES

- [1] N. M. Tang, K. Arslan, A. Shakeel, M. Palash, K. Imrana I, H. Y. Guan, P. B. Toan, L. W. Khoi, "Electrical tracking, erosion and flammability resistant of high voltage outdoor composite insulation: Research, innovation and Future outlook", *Materials Science and Engineering*, 2023, PP. 1-20.
- [2] Y. Xuerong, S. Ying, T. Yujing, H. Liping, R. Minqiao, Z. Cui, L. Li-zhi, "CRYSTAF, DSC and SAXS study of the co-crystallization, Phase Separation and Lamellar Packing of the blends with different polyethylenes", *Polymer Composite analysis and characterization*, *Polymers* 2023, PP: 1-21.
- [3] N. Dorottya, W. Zoltań, "Crystallinity and oscillatory Shear Rheology of Polyethylene Blends," *Materials*, 2023, PP:1-18.
- [4] V. Naidu M. Kamaraju, "High Voltage Engineering," *McGraw-Hill*, 2009.
- [5] O. I. Nkwachukwu and C. H. Chima, "Focus on potential environmental issues on plastic world towards a sustainable plastic recycling in developing countries," *International Journal of Industrial Chemistry*, vol. 4, 2013, pp. 34.
- [6] A. R. A. Raja, B. Vissauvanadin, T. T. N. Vu, G. Teysse, and N. I. Sinisuka, "Space Charge Measurement on XLPE Cable for HVDC Transmission using PEA Method", *Procedia Technology*, vol. 11, 2013, pp. 327-333.
- [7] F. Nilsson, M. Karlsson, U. Gedde, R. Kadar, K. Gaska, C. Miiller, P. O. Hasstrand, R. Ollson, M. Hedenqvist, and T. Gkourmpis, "Nanocomposites and polyethylene blends: two potentially synergistic strategies for HVDC insulation materials with ultra-low electrical conductivity," *Composites Part B: Engineering*, vol. 204, 2021, pp. 1-9.
- [8] L. Chunyang, J. Yongxing, S. Yuxuan, J. Duo, Y. Xu, S. Manzhi, Z. Hong, "Improved body and interface properties of EPDM insulation for HVDC cable accessory by grafted voltage stabilizer", *Surfaces and Interfaces* 54, 2024, pp. 1-14.
- [9] M. Ahmed, L. Zhong, F. Li, J. Gao, and H. Ren, "Simulation of Insulation Electrical Field of HVDC XLPE Cable Based on Radial Non-uniform Conductivity Distribution," *7th IEEE International Conference on High Voltage Engineering and Application (ICHVE)*, 2020, pp. 1-4.

- [10] N. Li, J. Chen, Z. Wang, P. Shen, and L. Zhou, "Electrical and material test of 200 kV HVDC XLPE cables after operating for 5 years," *7th IEEE International Conference on High Voltage Engineering and Application (ICHVE)*, 2020 pp. 1-4.
- [11] X. Anne, R. Sébastien, C. Xavier, "Physico-Chemical characterization of the blooming of Irganox 1076® antioxidant onto the surface of a silane-crosslinked polyethylene", *Polymer degradation and stability*, 2020, pp. 1-4.
- [12] W. Song, J. Tang, C. Pan, G. Meng, and M. Zhang, "Improvement of insulation defect identification for DC XLPE cable by considering PD aging," *International Journal of Electrical Power and Energy System*, vol. 114, 2020, pp. 1-9.
- [13] W. Yani, Y. Xingwu, M. Aiqing, and Y. Yi, "Simulation of Space Charge Distribution in the Insulation Layer of XLPE HVDC Cable under Different Temperatures," *International Symposium on Electrical Insulating Materials (ISEIM)*, 2020, pp. 1-5.
- [14] B. X. Du, Z. Y. He, Q. Du, and Y. G. Guo, "Effects of water absorption on surface charge and dielectric breakdown of polyimide/Al<sub>2</sub>O<sub>3</sub> nanocomposites films," *IEEE Transactions on Dielectrics and Electrical Insulation*, vol. 23, no. 1, 2016, pp. 3073-3082.
- [15] I. L. Hosier, M. Praeger, A. S. Vaughan, and S. G. Swinger, "The effects of hydration on the DC breakdown strength of Polyethylene composites employing oxide and nitride fillers," *IEEE Transactions on Dielectrics and Electrical Insulation*, vol. 24, no. 5, 2017, pp. 3073-3082.
- [16] B. X. Du, H. Xu, J. Li, and Z. Li, "Space Charge behaviour of PP/POC/ZnO nanocomposites for HVDC cables," *IEEE Transactions on Dielectrics and Electrical Insulation*, vol. 23, 2016, pp. 3165-3174.
- [17] L. Hui, L. Schadler, J. K. Nelson, "The influence of moisture on the electrical properties of crosslinked polyethylene/silica nanocomposites," *IEEE Transactions on Dielectrics and Electrical Insulation*, vol. 20, 2013, pp. 641-653.
- [18] K. Y. Lau, A. S. Vaughan, G. Chen, I. L. Hosier, and A. F. Holt, "On the dielectric response of silica-based Polyethylene nanocomposites," *Journal of Physics D: Applied Physics*, vol. 46, 2013, no. 9.
- [19] W. Callister and D. Rethwisch. *Materials Science and Engineering: An Introduction*, 10<sup>th</sup> Edition, In John Wiley & Sons, 2018, pp. 975.
- [20] A. Mayahadi and S. R. Jadar, "Structural, electrical and photo electrochemical properties of calcined SnO<sub>2</sub>/TiO<sub>2</sub> nanocomposites films for solar cell applications," In: *Proceeding-International Conference on Technologies for Sustainable Development*, 2015, pp. 5-8.
- [21] S. M. M. Yasin and S. Ibrahim. "Effect of zirconium oxide nanofiller and dibutyl phthalate plasticizer on ionic conductivity and optical properties of solid polymer electrolyte." *The Scientific World Journal*, 2014.
- [22] A. Azmi. "Structure and dielectric properties of polypropylene containing multi-element oxide nanofillers," PhD Thesis, Universiti Teknologi Malaysia, 2022.
- [23] I. L. Hosier, A. S. Vaughan, S. Swinger, "Structure-property relationships in polyethylene blends: the effect of morphology on electrical breakdown strength", *Journal of Materials science*, 1997, pp. 4523-4531.
- [24] N. H. Rahim, K. Y. Lau, N. A. Muhamad, N. Mohamad, W. A. W. A. Rahman, and A. S. Vaughan, "Effects of filler calcination on structure and dielectric properties of polyethylene/silica nanocomposites," *IEEE Transactions on Dielectric and Electrical Insulation*, vol. 26, 2019, no. 1, pp. 284-291.
- [25] I. L. Hosier, A. S. Vaughan, A. Pye, and G. C. Stevens, "High performance polymer blend systems for HVDC applications," *IEEE Transactions on Dielectrics and Electrical Insulation*, 2019, vol. 26, no. 4, pp. 1197-1203.
- [26] N. H. Rahim, K. Y. Lau, N. A. Muhamad, N. Mohamad, C. W. Tan, and A. S. Vaughan, "Structure and Dielectric properties of polyethylene nanocomposites containing calcined zirconia," *IEEE Transactions on Dielectrics and Electrical Insulation*, 2019, vol. 27, no. 5, pp. 1541-1548.
- [27] A. H. Zamani, R. Ali, and W. A. B. Wa, "CO<sub>2</sub>/H<sub>2</sub> methanation over M\*/Mn/Fe-Al<sub>2</sub>O<sub>3</sub> (M\*:Pd,Rh, and Ru) catalyst in natural gas, optimization by response surface methodology-central composite design," *Clean Technologies and Environmental Policy*, 2015, vol. 17 (3), pp. 627-636.